Atomistic modeling at experimental strain rates and timescales

IOP Publishing Journal of Physics D: Applied Physics

J. Phys. D: Appl. Phys. **49** (2016) 493002 (19pp) doi:10.1088/0022-3727/49/49/493002

Topical Review

Atomistic modeling at experimental strain rates and timescales

Xin Yan[1], Penghui Cao[2], Weiwei Tao[3], Pradeep Sharma[1] and Harold S Park[3]

[1] Department of Mechanical Engineering, University of Houston, Houston, TX 77204, USA
[2] Department of Nuclear Science and Engineering, Massachusetts Institute of Technology, Cambridge, MA 02139, USA
[3] Department of Mechanical Engineering, Boston University, Boston, MA 02215, USA

E-mail: psharma@uh.edu and parkhs@bu.edu

Received 29 January 2016, revised 19 September 2016
Accepted for publication 4 October 2016
Published 10 November 2016

Abstract

Modeling physical phenomena with atomistic fidelity and at laboratory timescales is one of the holy grails of computational materials science. Conventional molecular dynamics (MD) simulations enable the elucidation of an astonishing array of phenomena inherent in the mechanical and chemical behavior of materials. However, conventional MD, with our current computational modalities, is incapable of resolving timescales longer than microseconds (at best). In this short review article, we briefly review a recently proposed approach—the so-called autonomous basin climbing (ABC) method—that in certain instances can provide valuable information on slow timescale processes. We provide a general summary of the principles underlying the ABC approach, with emphasis on recent methodological developments enabling the study of mechanically-driven processes at slow (experimental) strain rates and timescales. Specifically, we show that by combining a strong physical understanding of the underlying phenomena, kinetic Monte Carlo, transition state theory and minimum energy pathway methods, the ABC method has been found to be useful in a variety of mechanically-driven problems ranging from the prediction of creep-behavior in metals, constitutive laws for grain boundary sliding, void nucleation rates, diffusion in amorphous materials to protein unfolding. Aside from reviewing the basic ideas underlying this approach, we emphasize some of the key challenges encountered in our own personal research work and suggest future research avenues for exploration.

Keywords: molecular dynamics, time scales, strain rate, potential energy surface

(Some figures may appear in colour only in the online journal)

1. Introduction: motivation for long timescale atomistic simulations

In 1934, G I Taylor made what is now a historical speculation: that atomistic defects called 'dislocations' are responsible for the ductile 'plastic' deformation of metals [1]. Were the scientists of that time to have had recourse to molecular dynamics (MD) algorithms and modern computers, this would not have been *mere* speculation, and direct evidence of dislocation-mediated plasticity would be at hand. This arguably artificial scenario underscores the power of conventional MD simulations to provide microscopic insights into material behavior that sometimes may not be easily discernible experimentally[4]. Indeed, conventional MD, which simply consists

[4] While MD simulations are of importance in a diversity of disciplines, such as chemistry, physics and biology among others, we will primarily focus on materials with a further emphasis on mechanical aspects.

of numerically solving the Newtonian equations of motion for a set of atoms, has unrivaled predictive power in providing a microscopic window to the chemical, mechanical and physical behavior of materials. MD can be used to elucidate atomistic structures and mechanisms that aid in the interpretation of the experiment, or even reveal behavior that is unavailable to test in a laboratory setting. Archival literature, and now even textbooks [2, 3], are rife with examples of the success achieved by MD in understanding physical phenomena from an atomistic viewpoint.

In principle, MD can be used to obtain any thermodynamic or kinetic quantity, without introducing approximations beyond the assumption of classical mechanics and what may be involved in deriving an interatomic potential. However, when we integrate the equations of motion $-\frac{dV}{dr_i} = m_i\frac{d^2r_i}{dt^2}$[5] in MD, the resolution of individual atomic vibrations requires an integration time-step of the order of femtoseconds (10^{-15} s). Even the fastest processors of our times can, at present, achieve total simulation times of microseconds (10^{-6} s). The time-integration is inherently sequential in nature, and accordingly, direct parallelization does not help much in resolving the 'timescale bottleneck' of conventional MD[6]. The timescale limitation of conventional MD restricts its usefulness to phenomena that occur within micro to nanosecond timescales. Thus, many interesting physical processes that occur at much longer timescales than microseconds, i.e. creep, diffusion, protein unfolding, grain boundary dynamics, etc, are inaccessible by conventional MD.

In the past, researchers have attempted simulation acceleration via application of higher temperatures [4], high stress [5], and high strain rate [6]. Unfortunately, all these treatments may conceal important behavior and mechanisms during deformation. Accessing long timescales in atomistics has therefore become an intensely studied research topic within the past decade, and notable success has been achieved using different approaches. Complete success, however, has still been elusive, and all approaches have their respective strengths and limitations. Among many, the autonomous basin climbing (ABC) method is one of the attempts to circumvent the timescale issue of traditional MD [7, 8]. This algorithm was originally applied to the study of supercooled liquids, viscosity, and glass transition (more details can be found in a previous review [8]). In this review, we provide a general summary of principles underlying the ABC approach, with emphasis on recent methodological developments enabling the study of mechanically-driven processes at slow (experimental) strain rates. We first, very briefly, review other long timescale atomistic approaches in section 2. The central concept of the ABC approach and other associated methods are described in section 3. In section 4, we survey a few representative case studies using ABC-based methods. Finally, based on our personal experience with the ABC approach, we outline some key issues, possible solutions and indicate some future directions.

[5] V is the interatomic potential.

[6] We remark, however, that parallelization has had a very positive impact on bridging lengths scales and thus now large system sizes consisting of billions of atoms can be handled.

2. A brief review of long timescale atomistic methods

Over the past few decades, there have been various attempts to extend the timescale of atomistic simulations beyond those that can be accessed with traditional MD. These approaches can be categorized into two groups. The first are those based on potential energy surface (PES) exploration, where different techniques are developed to efficiently explore the PES.

The second set of approaches can generically be grouped as accelerated MD approaches. In this category, different techniques are utilized to accelerate traditional MD, thereby extending the timescales that can be accessed using molecular simulation. Because this review is a focus on one particular long timescale method (ABC), our objective here is to provide a brief overview of representative methods in both categories, while noting that more comprehensive discussions on long timescale atomistic techniques can be found elsewhere, i.e. [9–11].

2.1. Potential energy surface exploration

A general approach to determining the evolution of an atomistic system without explicitly solving and integrating Newton's equations of motion is through PES exploration, where transition state theory (TST) provides a link between the time evolution of the system to the topology of the underlying PES. We show in figure 1 a one-dimensional PES with different local energy minima that can be accessed by climbing over the various energetic barriers $\Delta E_{(i)}$. In general, the PES is $3N$-dimensional, where N is the number of atoms in the system. Various approaches have been proposed that enable efficient and accurate exploration of the $3N$-dimensional PES.

One approach is metadynamics [12], which was originally developed as a free energy surface sampling technique, but has evolved to function as a general PES exploration technique that can resolve saddle points, local energy minima, and the connecting energetic barriers. Metadynamics works by adding Gaussian functions to the PES to force the system out of local energy minima and into neighboring energy wells. In order to reduce the infinite number of configurations that can be explored on the PES, metadynamics utilizes so-called 'collective variables', which are functions of the system configuration that are used to bias the PES search directions. Examples of such collective variables are coordination numbers, potential energies, box shapes, and path variables [13]. Metadynamics is limited in the number of atoms that can be modeled due to its need to store all previously used Gaussian functions, which is necessary to prevent the system from re-exploring previously found potential energy basins.

Other approaches to finding neighboring local minima, and thus to explore the PES, include the activation–relaxation technique (ART) [14, 15] and the dimer method [16]. ART is a method of searching the saddle points associated with a selected basin on the PES. ART works by applying a perturbation to a relaxed system, which forces the system up a potential energy well to locate the saddle point. The system is

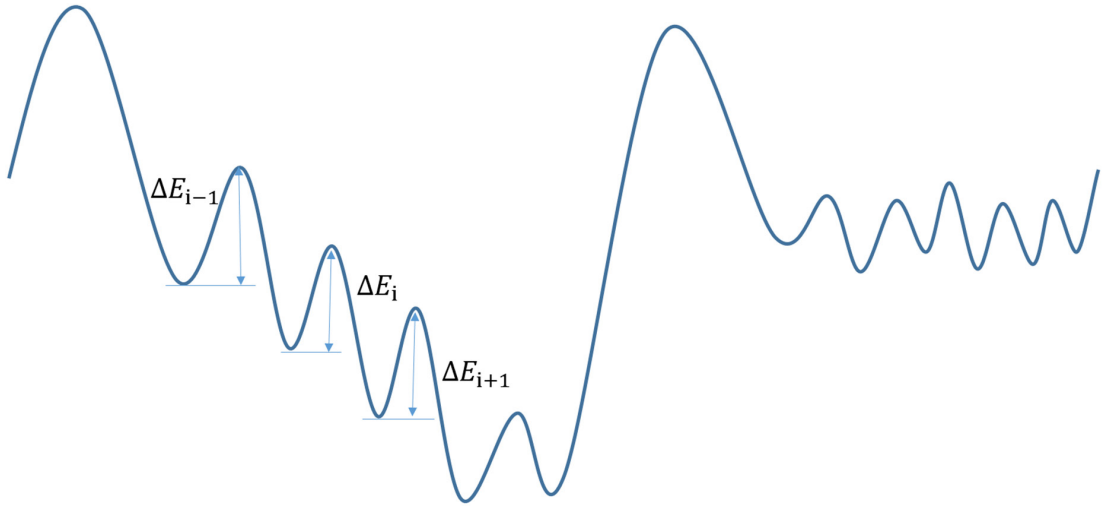

Figure 1. Schematic of a one-dimensional potential energy surface.

then set back to the relaxed energy minimum, at which point another perturbation is applied [14, 17]. ART has been used with success in various applications [18], but does exhibit shortcomings due to increasing computational expense for complex non-equilibrium processes, where it can encounter difficulties related to computational expense in finding a final, desired system configuration [19].

In the dimer method [16], one rotates a dimer (two replicas with constant distance) to find the lowest curvature mode of the PES at the current position. The approach subsequently forces the dimer to move up the PES along this direction to find the saddle point. Similar to ART, once a saddle point is reached, the system is set back to the original local energy minimum, and displaced along another random direction to find other saddle points.

The discrete path sampling method of Wales [20, 21] is another approach to PES exploration. This approach has been used, for example, for applications involving different aspects of protein folding and unfolding [22, 23]. The equilibrium mapping approach [24] uses branch-following and bifurcation algorithms to generate a diagram that contains information regarding the possible stable and unstable equilibrium states on the PES.

The approaches that have been discussed above all deal with finding a pathway between a specified initial configuration, and a resulting, generally unprescribed final configuration. Intrinsic to these PES exploration techniques is the fact that the concept of time, i.e. the real physical time a system would expend in going from the initial to the final configuration, is not addressed. Instead, the output of these PES exploration simulations is typically the energy barriers that have been crossed in going from the initial to the final configuration. Thus, once the pathway between two configurations on the PES has been determined, connections to time t can be made through TST [25, 26], i.e.

$$t = \sum_{i=1}^{N} (\nu \exp^{-\Delta E_i/k_b T})^{-1}, \quad (1)$$

where ΔE_i is the energy barrier separating energy minima $i-1$ and i, N is the total number of energy minima explored, ν is a frequency prefactor that is typically chosen to be on the order of 10^{12} s^{-1} for crystalline solids, T is the temperature and k_b is the Boltzmann constant. Through this TST connection, one can calculate the amount of time needed for a specific energetic transition to occur, or for the system to reach a specific final configuration.

An important comment to make is that equation (1) makes clear that the calculated time t needed to cross an energy barrier on the PES is dependent on the accuracy of the energy barrier ΔE_i. In other words, errors in computing this value may lead to either under or over prediction of the barrier crossing time. Due to this feature, besides methods that explore the PES by finding neighboring energy minima, methods exist that enable accurate calculation of each energy barrier that is crossed during the PES exploration. Perhaps the most widely used approach to calculating the value of the energy barriers by finding the minimum energy pathway (MEP) is the nudged elastic band method (NEB) [27]. One of the artifacts that plague ABC and other PES exploration methods is that often the saddle points are discovered in a sequence that is not physically relevant. Accordingly, it is usually necessary to employ a technique such as kinetic Monte Carlo (KMC). KMC can be applied to select the most probable path a system may take, starting from some initial minimum state to the various minima identified during the ABC-based PES exploration.

2.2. Extended timescale atomistic methods

Apart from PES exploration techniques, extensive efforts have been dedicated to accelerating traditional MD. Much of this effort has been performed by Voter and co-workers, who have developed a range of approaches to extend the timescale in MD simulations, including parallel-replica dynamics [11], hyperdynamics [28], and temperature-accelerated dynamics [9, 29].

In parallel-replica dynamics, the system is first replicated on M processors. Each replica is evolved forward independently using thermostatted MD. After a transition is detected in any of the replicas, the parallel simulations of all replicas are terminated, and the transition time can be calculated as the summation of the trajectory time over all replicas [30]. An extensive discussion of parallel-replica dynamics was recently given by Perez *et al* [11].

In hyperdynamics, a bias potential is added to the PES in the areas close to local minima. In this way, the height of the barriers between different states is reduced. A boost factor can be obtained due to the bias potential, which can be used to scale the transition time [28]. However, the bias potential must be zero at the dividing surfaces between two minima, and must also satisfy the constraint that the bias potential does not erroneously alter the dynamical evolution of the system, which introduces challenges and significant computational cost in effectively applying the bias potential in hyperdynamics applications. Because of this, other researchers have pursued different approaches to adding the bias potential. For example, in the accelerated MD approach, the bias potential is applied to the entire PES when the system potential energy is below a certain threshold, which has been used to study the configurational space of biological materials in an efficient manner [31]. Simple versions of hyperdynamics using local bias potentials, such as the bond-boost [32] and strain-boost [33] methods, have also been proposed to increase the efficiency and accuracy of hyperdynamic-type approaches, and recent approaches using hyperdynamics to study fracture in crystalline materials containing millions of atoms have recently been performed [34].

Temperature-accelerated dynamics accelerates the transitions by increasing the temperature in the MD simulation, after which an extrapolation to the low-temperature regime is performed assuming Arrhenius behavior while filtering out the transitions that could not have occurred at the required temperature [29]. While large time boosts can be achieved, the temperature-accelerated dynamics method appears to be most effective for systems where the lowest energy barrier of interest is relatively high [11].

A final point we would like to make before discussing the ABC method is that many of the PES or accelerated MD methods, and applications of the methods, have originated to solve problems involving diffusion, chemical reactions, glass transitions, etc, i.e. where mechanically-driven system evolution is not the primary physics of interest. In contrast, significantly fewer studies have been performed on mechanically-driven systems, i.e. when considering externally applied stresses or forces. It is this particular subset of long timescale applications that we intend to focus upon in this review.

3. ABC sampling method and ABC-based approaches

3.1. Original ABC PES sampling method

The ABC method was originally proposed by Yip *et al* in 2009 [7, 35]. It has since been applied to a wide range of phenomena which require atomistic resolution at timescales far beyond those accessible via traditional MD, including trapped self-interstitial atom clusters [36], strain-rate effects on yield stress [37], interstitial emission at grain boundaries [38], diffusion [19], and viscous relaxation [8]. The original ABC method, which is an activation–relaxation method used to explore and reconstruct the PES, is illustrated in figure 2. Specifically, the ABC PES sampling process involves the following steps:

I. An initial structure at an energy minimum, i.e. $E^{(1)}_{\rm min}$ in figure 2(a), is chosen.
II. A penalty function $\phi_i(\mathbf{r})$ with a particular shape is added to the system, where i denotes the local penalty function number. The width and height of the penalty functions determines the sampling resolution of the PES; these parameters are often dependent on the specific physical problem of interest, as discussed later. The penalty functions typically assume Gaussian-like shapes, i.e.

$$\phi_i(\mathbf{r}) = \omega \exp[-(\mathbf{r} - \mathbf{r}^i_{\rm min})^2/2\sigma^2], \tag{2}$$

which are centered at the minimum energy configuration $\mathbf{r}^i_{\rm min}$. The parameters ω and σ control the strength and width of the penalty function. These penalty functions modify the potential energy $\Psi(\mathbf{r})$ as

$$\Psi(\mathbf{r}) = E(\mathbf{r}) + \sum_{i=1}^{p} \phi_i(\mathbf{r}), \tag{3}$$

where $\mathbf{r}$ are the $3N$-dimensional atomic configurations and p is the total number of penalty functions.
III. The system is relaxed using static energy minimization (i.e. using conjugate gradient energy minimization) to find the next minimum energy configuration $\mathbf{r}^{i+1}_{\rm min}$ on the penalty function-modified PES.
IV. Repeat starting from step II until the target physical phenomenon is observed.

The above outline and figure 2 make clear that there are similarities and differences with metadynamics [12, 13]. For example, metadynamics was designed as a dynamic sampling tool for exploring the free energy surface. In contrast, the ABC method is limited to the PES exploration method as static energy minimization is used to relax the system between penalty function increments. Another key difference is that the penalty functions in metadynamics are typically constrained by a choice of collective variables [12]; these are used because of the computational expense inherent in considering entropic effects, and also to reduce the dimensions of the free energy landscape search. In contrast, the ABC method does not utilize collective variables, and thus represents an unconstrained PES search methodology. The practical implications of this difference are that the ABC method can, in theory, find all transitions on the PES, though not all of them may be important or relevant, whereas metadynamics will only find those transitions that are of relevance to the collective variables.

The discussion above corresponds to the original ABC method of Kushima *et al* [7, 35]. Since 2009, multiple groups, including those involved with this review article, have identified and attempted to ameliorate deficiencies that have been identified with the basic ABC PES exploration method. These issues

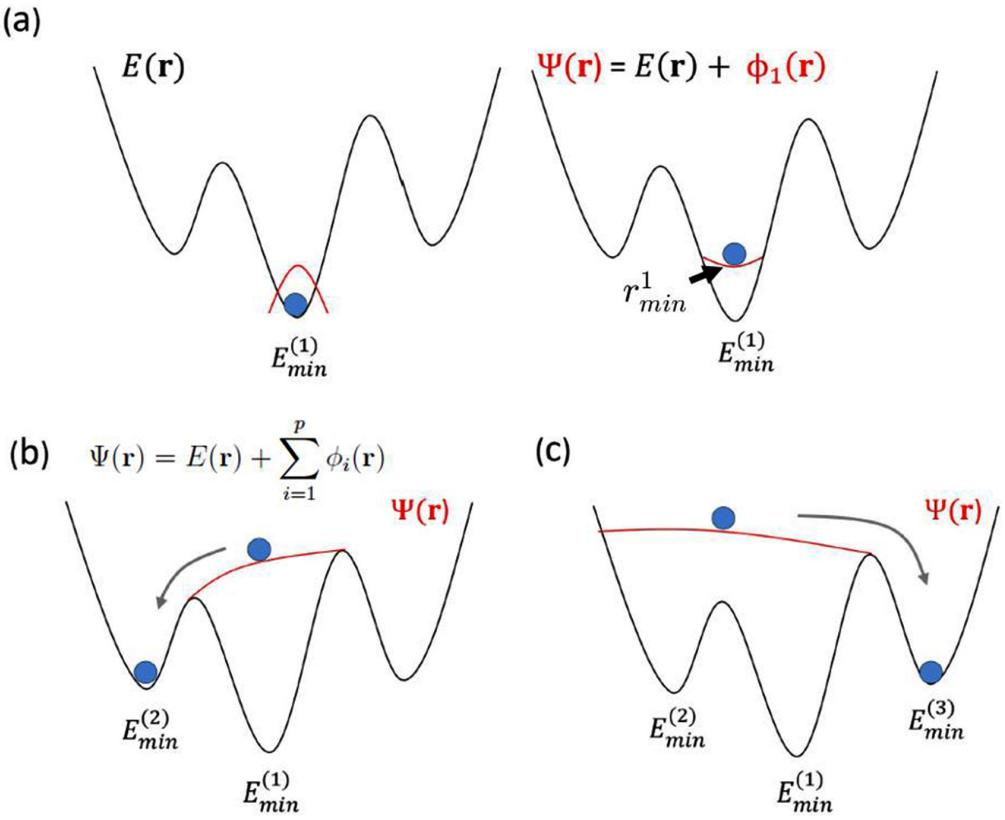

Figure 2. Illustration of basin filling with penalty functions in the ABC method. (a) Penalty function ϕ_1 added to PES, with the center of the penalty functions at $\mathbf{r}^i_{\min}$; ((b) and (c)) continue adding additional penalty functions to push the system to neighboring energy wells. Adapted from [39] with permission. Copyright 2014 Elsevier.

include: (1) computational expense related to storing penalty functions for PES exploration; (2) resolving the one-dimensional nature of the PES search that is intrinsic to the ABC method; (3) improving the accuracy of energy barriers obtained through the ABC PES exploration; (4) choosing the most probable ABC pathway or trajectory. We now describe each of these in detail.

3.2. Self-learning metabasin escape algorithm

One of the key computational bottlenecks facing the basic ABC method is the increasing number of penalty functions that must be stored as more and more of the PES is explored. The reason for this is illustrated in figures 2(b) and (c). Specifically, in figure 2(b), a sufficient number of penalty functions are applied such that the system exists in the energy well defined by the minimum $E^{(1)}_{\min}$, and into the neighboring energy well defined by the local minimum $E^{(2)}_{\min}$. Additional penalty functions are applied to the energy well with $E^{(2)}_{\min}$ until the system is able to exit to the neighboring energy well with minimum $E^{(3)}_{\min}$. In going from $E^{(1)}_{\min}$ to $E^{(3)}_{\min}$, all of the penalty functions that are applied need to be stored, or else the system could fall back into the energy well containing the local minimum $E^{(1)}_{\min}$ in going from $E^{(2)}_{\min}$ to $E^{(3)}_{\min}$. In general, keeping previously applied penalty functions are necessary to prevent the system from falling into and re-exploring energy basins that have already been explored, though this means that the computational expense associated with the PES search increases dramatically as more of the PES is explored.

To mitigate this problem, Cao *et al* [40] formulated a self-learning strategy to improve the PES exploration efficiency, termed the self-learning metabasin escape (SLME) method. Starting from an initial configuration that is a local energy minimum, a small random penalty function is applied to the system. Starting from the second penalty function, after adding each penalty function to the system, an overlap check is carried out. If the distance between the center of the newly added penalty function and any of the previous penalty functions is less than the sum of their half-widths, these two penalty functions will be replaced by a new, single penalty function with a height equal to the sum of the two penalty functions and a width of $\boldsymbol{W}_n$, which can be written as [40]

$$|\boldsymbol{W}_n| = \max\left[\frac{|\boldsymbol{s}_i - \boldsymbol{s}_j| + |\boldsymbol{W}_i| + |\boldsymbol{W}_j|}{2}, |\boldsymbol{W}_i|, |\boldsymbol{W}_j|\right]. \quad (4)$$

The center of the new penalty function will be shifted to

$$\boldsymbol{s}_n = \frac{|\boldsymbol{W}_i| h_i \boldsymbol{s}_i}{|\boldsymbol{W}_i| h_i + |\boldsymbol{W}_j| h_j} + \frac{|\boldsymbol{W}_j| h_j \boldsymbol{s}_j}{|\boldsymbol{W}_i| h_i + |\boldsymbol{W}_j| h_j}. \quad (5)$$

In the expressions above, $\boldsymbol{s}$ and h represent the center and the height of the penalty functions, respectively. The new penalty function will be treated as the current penalty function, and the previously identified two overlapping penalty functions

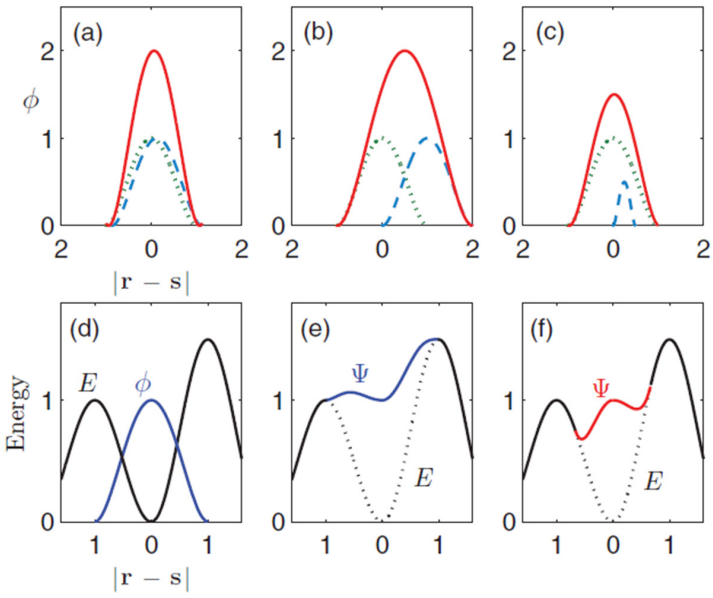

Figure 3. (a) Two sequential fully overlapping penalty functions (green, dotted curve and blue, dashed curve) give a strong indication of inefficient sampling. The combined penalty function (red, solid curve) doubles the local curvature to assist the system in moving away from the stuck configuration. (b) Combination of two penalty functions (green, dotted and blue, dashed curves) at the maximal separation. The new penalty function (red, solid curve) has a half-width that is 3/2 times that of the original values. (c) The combination between two penalty functions of different sizes. (d) The original energy E and the penalty function ϕ with self-learned half-width $|\mathbf{w}|=|\mathbf{s}_{\rm sad}-\mathbf{s}|$ and height $h=E(\mathbf{s}_{\rm sad})-E(\mathbf{s})$. (e) Their augmented energy Ψ still has a dip at the original local minimum. (f) The augmented energy Ψ using a smaller half-width $|\mathbf{w}|=\frac{2}{3}|\mathbf{s}_{\rm sad}-\mathbf{s}|$, curves downwards, which is desirable for fast relaxations. Reprinted with permission from [40]. Copyright 2012 by the American Physical Society.

can then be removed from memory. Figure 3 demonstrates three typical cases of how overlapping penalty functions can be combined, i.e. (a) two largely overlapping penalty functions; (b) two slightly overlapping penalty functions; (c) the combination of a larger and smaller penalty function. The SLME approach was shown to lead to significant decreases in computational expense, thus enablings the ABC method to find significantly more local energy minima on the PES in a shorter amount of time, as shown by Cao *et al* [40].

3.3. Extended ABC (ABC-E)

Another modification of the basic ABC algorithm was developed by Fan *et al* [19] which is called the extended ABC (ABC-E). In ABC-E, after a new energy basin is identified, the system is sent back to the initial energy basin and a Gaussian penalty function is added on the saddle point to block the identified pathway. Penalty functions are then added until another saddle point is found, at which point the system is again placed back into the initial energy basin while the newly found saddle point is blocked with penalty functions. In this way, a series of distinct exits or transition pathways from a single energy basin can be identified. Identifying the exit pathways in order of the increasing activation barrier enables them to be sorted according to their relative importance and contribution to the process kinetics.

Thus, the ABC-E, and the ABC–SLME represent the two major algorithmic improvements to the original ABC method. Aside from the distinctions already discussed, another key difference between them is that ABC-E may provide more accurate estimations of transition time because it is not a one-dimensional PES searching tool [19], in contrast with the ABC–SLME. However, there exists a trade-off in computational expense, with ABC-E being more expensive than ABC–SLME. This, and the other choices discussed above, leads to trade-offs in terms of sampling rigor and computational efficiency, which are summarized in table 1.

3.4. Rate constants

Regardless of the specific ABC PES methodology that is utilized, the output from an ABC PES search are all the energy barriers that are crossed, as well as all of the local energy minima. However, one shortcoming that is intrinsic to all of the discussed ABC methods is an overestimation of the energy barriers connecting neighboring energy minima, which thus causes an overestimation of the corresponding transition times. One approach to mitigating this issue is to utilize penalty functions with smaller heights. However, this requires more penalty functions to exit a given local energy well, and thus results in significantly enhanced computational cost. Alternatively, minimum energy pathway strategies, which are superior in calculating energy barriers, such as the NEB [27] and finite temperature spring (FTS) [41, 42], can be adopted. After refining the energy barriers obtained from ABC using NEB or FTS, the transition times can be calculated through TST using equation (1).

Table 1. Comparison of different ABC PES sampling approaches.

	Original ABC [7]	ABC-E [19]	ABC–SLME [40]
Simple description	Starting from current energy minimum, Gaussian penalty functions are added to push the system to climb out of the current energy well	After a new minimum is identified using ABC, a penalty function is added on the saddle point to block the identified path. The system is then set back to the initial state to find other possible transition pathways out of the energy basin	If the new added penalty function overlaps with existing ones, the overlapping penalty functions will be replaced by a new, larger one
NEB is used to accurately calculate the energy barriers	Yes	Yes	No
Sampling efficiency	Intermediate	Slowest	Fastest
Time estimation	Less accurate	More accurate	Less accurate

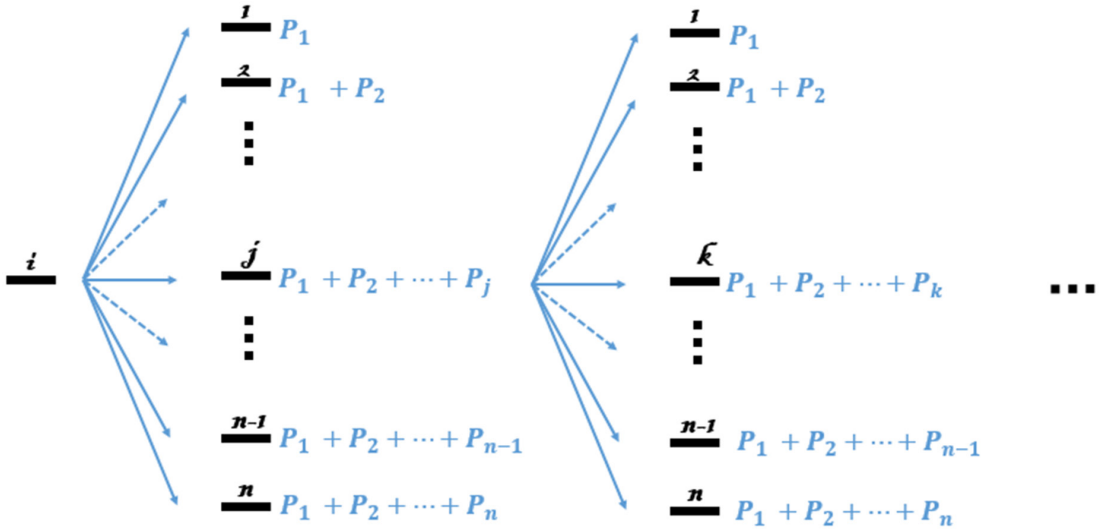

Figure 4. KMC algorithm: Starting from the state i, a random number (r) in the range of (0,1] is compared with the partial summation of possibilities and it turns out $P_1 + P_2 + ... + P_{j-1} < r < P_1 + P_2 + ... + P_j$. Thus,the system will jump to state j. State j become the current state and the same action will be taken with state j. Reprinted from [43] with permission. Copyright 2015 Elsevier.

However, the ABC PES searches are not deterministic in the sense that starting from the same local energy minimum on the PES, different ABC trajectories based on different parameters, namely the penalty function width σ and strength ω, may identify different minimum energy pathways, or different sequences of local energy minima. Thus, KMC [26] is used to ascertain the most probable pathway that the system follows in going from one physical state to another. This method is used to calculate the corresponding possibilities for the system to cross every barrier (that has been identified) and to determine the most probable transition trajectory to cross the various energy barriers. With all the barrier information calculated from ABC or an MEP method like NEB, TST is then applied to estimate the rate constant for each event (crossing a barrier):

$$k_{ij} \propto \exp[-\Delta E/k_b T] \tag{6}$$

where k_{ij} is the rate constant for the single event, ΔE is the barrier energy calculated from ABC/MEP, k_b is Boltzmann constant, and T is the temperature. The rate constant divided by the summation of the rate constants of all possible events from the current state yields the possibility of this single event. One of the possible transitions is randomly chosen based on the relative possibilities by comparing a randomly generated number in the range of (0,1] to an array of partial summations of the possibilities, as illustrated in figure 4. Starting from the new state, with the corresponding rate constants in the rate matrix, the same action is taken to find the next transition state.

We hope that the preceding discussion has demonstrated that the best strategy for extracting useful information from numerical simulations is to use several tools synergistically, while exploiting the advantages of each. In this respect, ABC is complementary to other techniques, such as MEP searches, harmonic transition state theory, and KMC, which are less efficient in PES sampling, but advanced in terms of detailed analysis of the transition pathways. We note that while significant advances in ABC methodology have emerged, there still exist key limitations of the ABC method; these will be discussed in further detail in section 6.

4. ABC for slow strain rate and long timescale atomistic simulations

As previously discussed, in conjunction with other techniques, the ABC method has shown substantial promise in studying atomistic processes that occur at long timescales. However, an important area that has, until recently, remained underdeveloped and underexplored is the specific question of how the ABC method of PES exploration can be utilized to study problems in which constant forces, or mechanical loading, are applied, or where the strain rate ($\dot{\epsilon}$) that is applied to the system is on laboratory timescales, i.e. $\dot{\epsilon} \approx 10^{-2}$ s^{-1}, and where the total amount of time that needs to be simulated is on the order of seconds or longer. In this section, we describe multiple methodologies that have recently emerged that use the ABC PES exploration method as an essential component to performing atomistic modeling at experimental strain rates and timescales.

4.1. Method 1: no mechanical loading or constant stress loading

The first approach can be used to study atomistic systems without loading or with constant stress [43, 44]:

I. For a given set of boundary conditions, the ABC method is used to sample the PES—this determines the local energy minima of the PES as well as the saddle points, thus yielding the energy barriers between different local minima.
II. The energy barriers obtained from ABC are approximate since the determination of the saddle points can be in error based on the resolution of the ABC sampling. Accordingly, to extract accurate energy barriers, NEB is applied to *all* of the pairs of local energy minima that are obtained from the ABC PES search.
III. With the energy barriers in hand, KMC is used to find the most probable pathway between the different PES minima.
IV. Following the pathway provided in step III, TST is used to calculate the transition time between two steps.

This approach uses the ABC method to find the pathway between the initial and final configurations, but exploits other techniques to get accurate energy barriers, and thus accurate transition times that are needed to move from one local energy minimum to another. This approach can thus be used to find processes that occur at timescales slower than those accessible to classical MD, but cannot be used for problems where the external loading is a prescribed strain rate.

4.2. Method 2: ABC–SLME method with constant clamping forces

A different set of mechanical boundary conditions that is important to model for long timescale simulations is that of a constant clamping force. Clamping forces are most often used in steered MD (SMD) studies of protein unfolding to mimic the experimental approach of applying forces to proteins via optical tweezers, or an atomic force microscope [45–49]. The methodology described here has been used in conjunction with the ABC–SLME approach to sampling the PES to study the mechanically-driven unfolding of various proteins [50–52].

I. Apply constant force to specific parts of the molecular system, i.e. the termini of a protein.
II. Apply a penalty function, followed by an energy minimization.
III. Repeat step II until the protein has unfolded.

The reason this approach is able to access the experimentally observed unfolding times of seconds is due to the continued application of penalty functions, where it is important to note the utility of the ABC–SLME approach here in enabling the PES exploration by significantly reducing the memory requirements for storing penalty functions in previously explored portions of the PES. In other words, for the small clamping forces that are applied (100 pN or smaller), the protein is likely to become stuck in various potential energy basins, and would remain stuck if it were not for the applied penalty functions. The penalty functions which are continuously applied to boost the system out of energy basins can be interpreted as thermal activation that assists the mechanical (clamping) force in enabling the system to escape from energy wells that it would otherwise become stuck in. The heights of all energy barriers ΔE_i that are crossed over can be used in equation (1) to determine the total unfolding time.

4.3. Method 3: ABC-E combined with on-the-fly KMC

The ABC-E method was designed for problems, such as diffusion, in which there are multiple competing physical processes, and thus energetic pathways on the PES, that are connected to the same energetic configuration. The ABC-E method can be applied to identify the competing states around the initial state [19]. The simulation steps are shown in the flowchart in figure 5, where the detailed description is as follows:

I. Starting from a local energy minimum, ABC is used to find a neighboring energy well.
II. Record the newly found state, and apply a large penalty function on the saddle point and set the system back to the previous minimum energy configuration just prior to crossing the saddle point.
III. Continue ABC to find another connected energy basin.
IV. Judge whether a new state or a previously visited state is found: (a) if it is a new state, calculate the possibility factor $\alpha(T)$ (the possibility factor $\alpha(T) = \frac{\exp\left(-\frac{E^{\text{new}}}{k_b T}\right)}{\sum_{N_{\text{states}}^{\text{obs}}} \exp\left(\frac{-E_i^{\text{obs}}}{k_b T}\right)}$; in this equation, E^{new} is the energy of a newly identified barrier and E_i^{obs} is the energy of the observed barriers), if $\alpha(T) < \alpha(T)_0$, stop sampling, otherwise go to step II; (b) if it is a previously visited state, put the system back to the previous state and add an additional blocking penalty on the saddle point. Restart step IV.

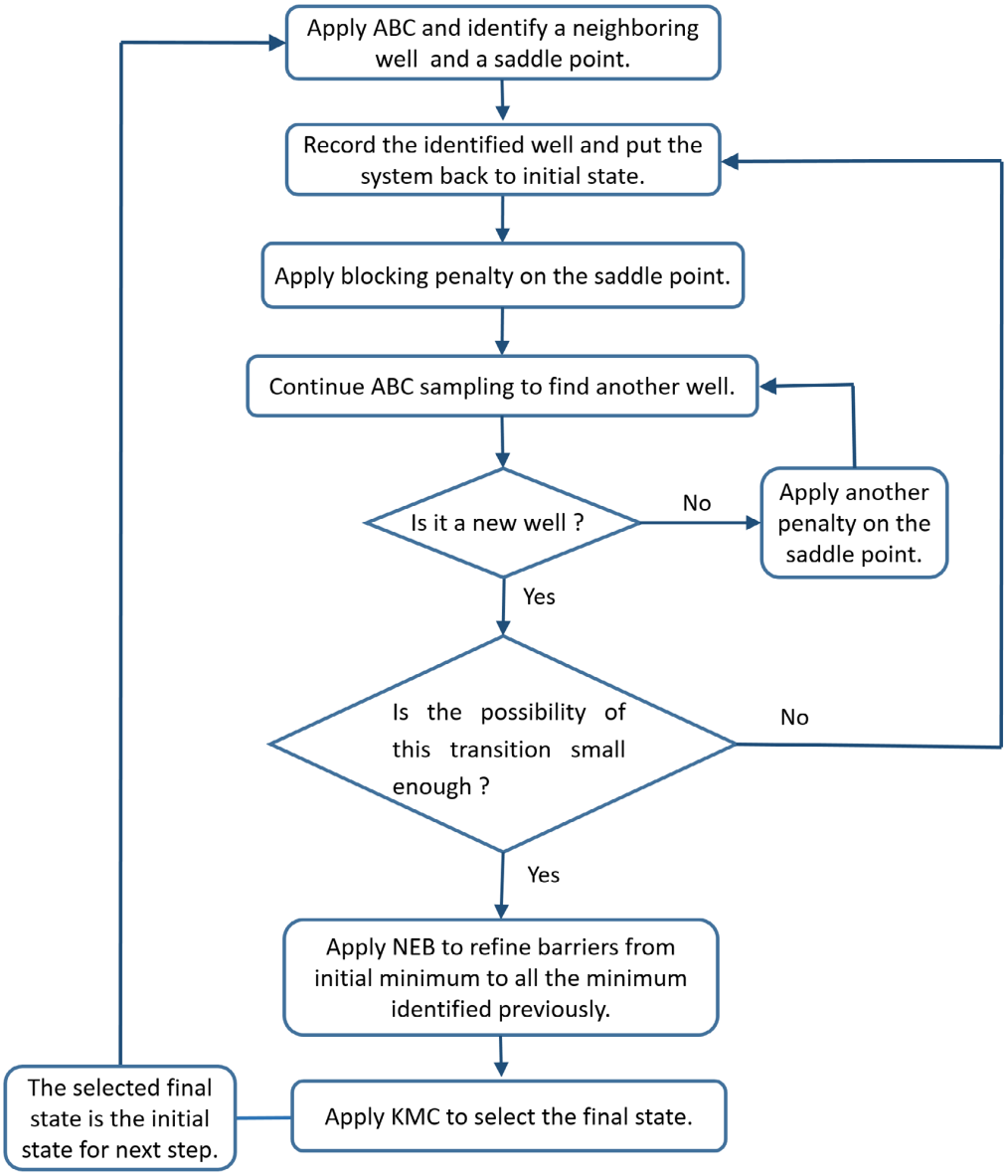

Figure 5. Algorithmic flowchart of method 3 (ABC-E) [19].

V. Apply NEB to refine all the saddle points identified in the ABC sampling.
VI. Apply KMC to select one final transition state from all the states identified in ABC.
VII. Starting from the selected state, go back to step I.

4.4. Method 4: Controlling strain rate via connection to the PES

In many problems in which the mechanical properties of atomistic systems are studied, a constant, but unrealistically large strain rate is applied [53–55]. To incorporate the effects of strain rate, Cao *et al* [39, 56, 57] proposed an approach coupling the ABC–SLME method with Monte Carlo, as illustrated in figure 6. In this approach, the connection between the strain rate and the energy barriers crossed on the PES is obtained by utilizing an expression for strain rate [58] that was derived from transition state theory assuming constant temperature:

$$\dot{\gamma} = n\nu_0 \frac{k_b T}{\mu \Omega} \exp\left[-\frac{Q^*(T) - TS_c}{k_b T}\right], \tag{7}$$

where n is the number of independent nucleation sites, ν_0 is the attempt frequency, μ is the shear modulus, Ω is the activation volume, Q^* is the energy barrier and S_c is the activation configurational entropy, which has previously been calculated, for example, for crystalline FCC metals for the specific case of dislocation nucleation [59].

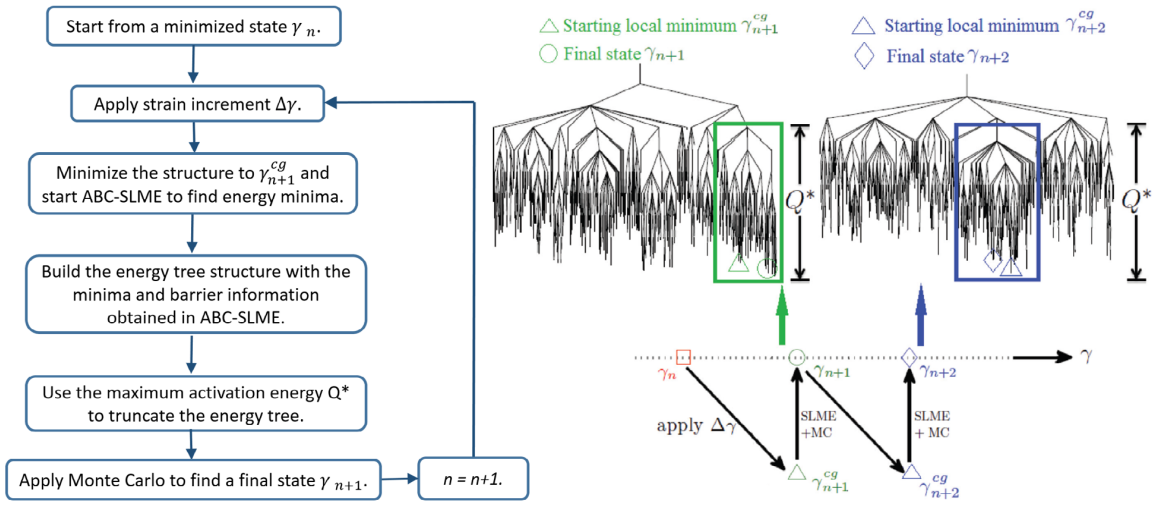

Figure 6. Algorithmic flowchart of the constant strain rate approach of Cao *et al* [39, 56]. Reprinted with permission from [56]. Copyright 2013 by the American Physical Society.

Then, by defining a characteristic temperature-dependent prefactor $\dot{\gamma}_0(T) = \frac{k_b T n v_0}{\mu \Omega} \exp\left(\frac{S_c}{k_b}\right)$ [60, 61], we can rewrite equation (7) as

$$\dot{\gamma} = \dot{\gamma}_0 \exp\left[-\frac{Q^*(T)}{k_b T}\right]. \tag{8}$$

Equation (8) thus plays the essential role of being a physical link between the SLME trajectories and the strain rates from MD to experimental values, which depends on only a single unknown temperature-dependent prefactor $\dot{\gamma}_0(T)$.

The connection between energy barriers, the PES, and enabling the study of atomistic systems at slow, constant strain rates is illustrated in figure 6, and its connection to the way in which deformation is applied experimentally to structures can be understood as follows. Experimentally, constant strain rate loading is performed by deforming the structure, and then waiting a certain amount of time before applying the next load increment, during which the system is able to relax. For high strain rate loading, the relaxation time given to the system before another deformation increment is applied is minimal. Thus, the system has only a small amount of time to explore its PES, implying that it will only be able to cross small energy barriers Q^* between each deformation increment. In contrast, for slow strain rate loading, the system has more time to explore its PES between loading increments, and thus may be able to climb over larger energy barriers Q^*. The ability to cross over large energy barriers Q^*, and thus access slow, experimentally-relevant strain rates, is made possible by the development of the ABC–SLME algorithm for efficient PES exploration [40].

The method can be detailed, as illustrated in figure 6 as:

I. Begin from a relaxed structure with strain γ_n.
II. Apply a strain increment $\Delta\gamma$.
III. Minimize the structure using conjugate gradient energy minimization while keeping the strain fixed. The system is then in the state γ_{n+1}^{cg}.
IV. Starting from the minimized state γ_{n+1}^{cg}, ABC–SLME is used to determine the potential energy tree structure, as shown in figure 6. The tree structure is truncated to only enable energetic transitions below Q^*, as shown in the green box in figure 6.
V. A Monte Carlo algorithm is employed to find the most likely equilibrium configuration (γ_{n+1}), at which point the algorithm repeats itself until a desired amount of strain has been applied to the system.

It is important to note that the PES is strain-dependent, and thus changes after each strain increment is applied. This is captured in this method, as shown in figure 6, by repeating the PES exploration after each new strain increment is applied.

4.5. Method 5: strict strain-rate controlled ABC

An alternate approach to applying a constant strain rate to an atomistic system was recently proposed by Fan *et al* [62]. The steps in this approach, as outlined in figure 7, are:

I. Choose a desired strain rate($\dot{\varepsilon}$).
II. For a given strain (ε_i), the current PES is sampled by ABC and a neighboring energy basin is identified.
III. NEB is then used to accurately calculate the energy barrier connecting the two energy wells.
IV. TST is used to calculate the transition time (Δt_i) between the initial and final states using equation (1).
V. The transition time (calculated in the previous step via equation (1)) is multiplied by the prescribed strain rate $\dot{\varepsilon}$ to find the corresponding strain increment $\Delta\varepsilon_{i+1} = \dot{\varepsilon}\Delta t_i$.
VI. Apply the strain increment ($\varepsilon_{i+1} = \Delta\varepsilon_{i+1} + \varepsilon_i$) to the system and go back to step II.

It should be noted that the strain in method 5 is being imposed on the system in discrete steps of variable magnitude depending on the height of the energy barrier that is found, and thus multiple PES' are identified rather than a single one. As discussed by Fan *et al* [62], errors could emerge if the

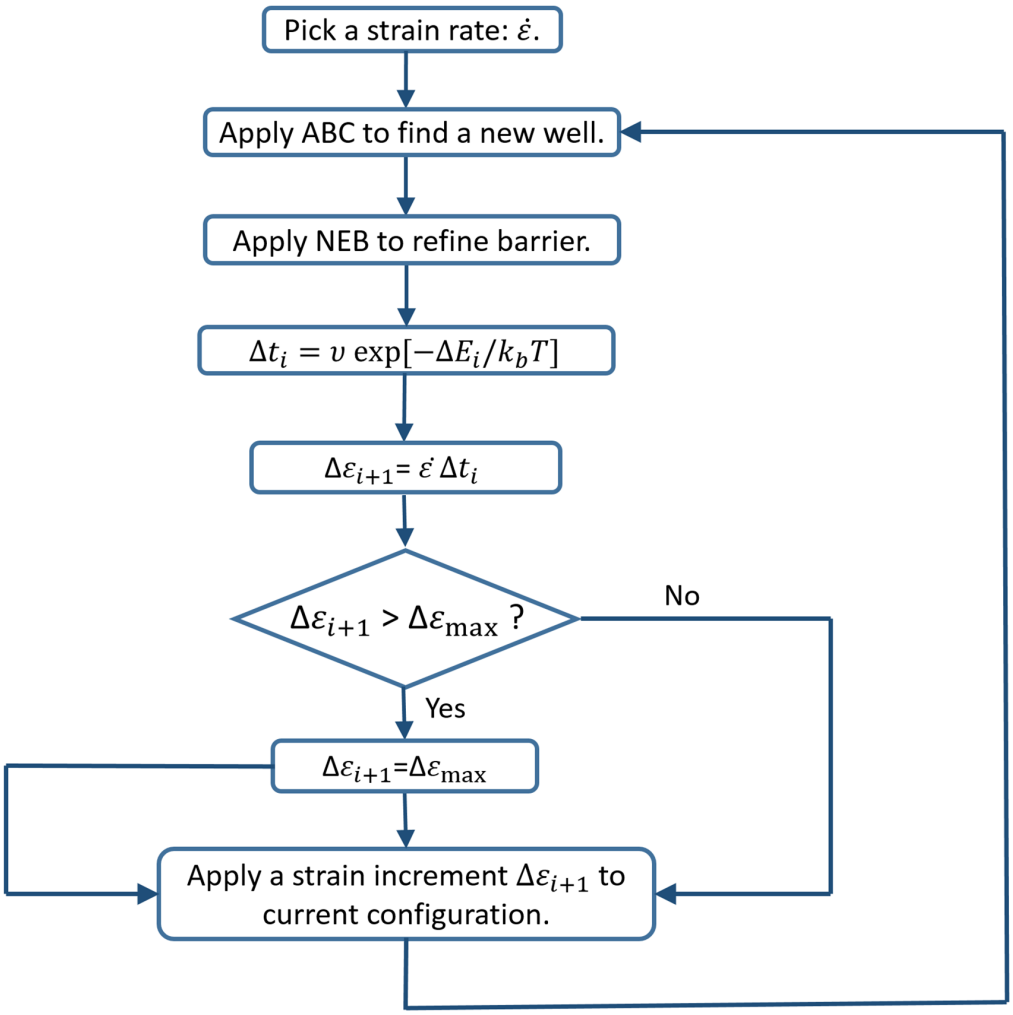

Figure 7. Algorithmic flowchart for method 5 [62].

calculated strain increment $\Delta\varepsilon$ is too large. This is because, in essence, the calculation steps are reversed from method 4 in that the strain increment is calculated based on the energy barrier that is crossed, rather than finding the new energy barrier based on the specified strain increment. Because of this reversal, only small strain increments can be applied to the system. Using increments that are too large would lead to errors because of the corresponding changes to the underlying PES.

Thus, because method 5 is restricted to smaller strain increments, it is more computationally expensive than the approach in method 4. This is not particularly problematic at fast, MD-accessible strain rates, but can introduce computational challenges at smaller strain rates due to the fact that, as seen in equation (1), crossing larger energetic barriers ΔE would lead to very small time increments Δt, which means that many strain increments are needed to deform the system an appreciable amount for slower strain rates. However, this approach ensures that the strain increment applied in the next step fits the defined strain rate.

On the other hand, method 5 is likely to be more accurate in its calculations of time than method 4 for two reasons. First, the use of NEB in method 5 results in accurate calculation of the height of the energy barriers that are crossed, which leads to more accurate calculations of the time spent climbing each energy barrier, as the NEB was not used by Cao *et al* [39, 56] in their development of method 4. Second, the strain increments are calculated based on the prescribed strain rate, such that the strain rate is accurately controlled.

An additional point to note is that both methods 4 and 5 currently assume that the prefactor that is used in equation (1) is a constant that is independent of strain. This is likely to cause some errors in the strain rate simulations, as other researchers have shown that the prefactors are not constant, and in fact can be calculated directly from information that can be obtained during the PES exploration. Such work has been performed recently by Stevenson and Wales [63, 64].

To conclude this section, in our opinion no approach is at present clearly superior than another in dealing with long timescale problems. Furthermore, physical intuition about the

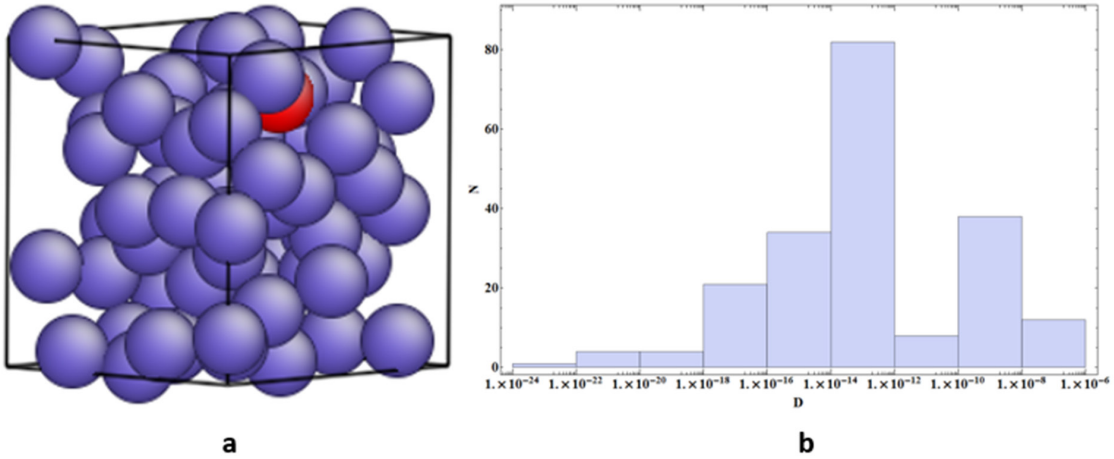

Figure 8. (a) Diffusion of a Li atom in a Si matrix; (b) resulting diffusion coefficient distribution. Reprinted from [43] with permission. Copyright 2015 Elsevier.

problem of interest is clearly beneficial to both choosing an approach and understanding the results obtained. In the next section, we give examples of recent studies based on the ABC approach that deal with various long timescale problems.

5. Applications of ABC—a review of some representative case studies

After its introduction in 2009, the initial applications of the ABC method were in the study of the viscosity of two types of supercooled liquids, SiO_2 and a binary Lennard–Jones (BLJ) system [7, 35]. Soon thereafter, Lau *et al* [65, 66] applied this approach to study the deformation in solids under constant strain mechanical loading. These initial efforts were reviewed in a recent review article [8]. Given the aforementioned review, we will not discuss these early applications of ABC any further, and instead focus on more recent examples that are predicted on the slow strain-rate methodologies described in section 4. Further simulation details of interest, i.e. interatomic potentials utilized and their physical justification, can be found in the specific references for each application below.

5.1. Applications of method 1: diffusion and grain boundary sliding

Yan *et al* [43] and Gouissem *et al* [44] used method 1 described in section 4 to address two problems: diffusion in amorphous materials and grain boundary sliding. Diffusive transport of Li-ions in the silicon (Si) anode is one of the key mechanisms that controls the deformation during lithiation, the rate of the charge–discharge cycle, and eventual mechanical failure. The atomistic mechanisms underpinning the diffusive transport of Li-ions in amorphous Si are, however, poorly understood. Conventional MD, if used to obtain atomistic insights into the Li-ion transport mechanism, suffers from several disadvantages; in particular, the relaxation times of Li ion diffusion in many of the diffusion pathways in amorphous Si are well beyond the short timescales of conventional MD.

Yan *et al* [43] studied Li diffusion in both an amorphous (figure 8) and crystalline (not shown in the figure) Si matrix. These simulations were performed by implementing the ABC algorithm into the open-source atomistic simulation code LAMMPS [67] such that the well-developed parallel computing capabilities and extensive interatomic potential database of LAMMPS could be employed in the ABC PES exploration, and the diffusion coefficients of Li in both crystalline and amorphous Si were evaluated. For crystalline Si, the diffusion pathway and diffusion coefficient matched prior density functional theory calculations. For amorphous Si, after ABC sampling, 257 minima were found. NEB calculations between every two minima were carried out and a 257×257 barrier matrix, which contains the energy barrier between all pairs of local energy minima, was generated, after which KMC was applied to find the most probable diffusive pathway at 300 K [43]. The most probable diffusive pathways naturally emerge from this approach, and the diversity of diffusivities obtained in the experiments can be replicated, as shown in figure 8(b).

Grain boundary sliding is the key deformation and damage mechanism for high temperature deformation of crystalline materials, thus impacting applications ranging from nuclear reactors to aircraft. Despite decades of research, both theoretical and experimental, a definitive atomistic understanding of this phenomenon has been elusive. To date, there is only speculation regarding the constitutive behavior of grain boundary sliding. Clearly, for such a rate-dependent process, MD is of limited use, and while the overall creep behavior can be determined experimentally, the specific constitutive response of grain boundary sliding appears to be unknown. Gouissem *et al* [44] applied method 1 to study grain boundary sliding in a bi-crystal under constant stress with the objective of developing physically reasonable constitutive laws based on atomistic simulations. In particular, that work aimed to answer important questions such as (i) is there a threshold stress for grain boundary sliding? and (ii) what is the form of constitutive law for grain boundary sliding? The simulation setup is shown in figure 9(a), where a constant shear stress is

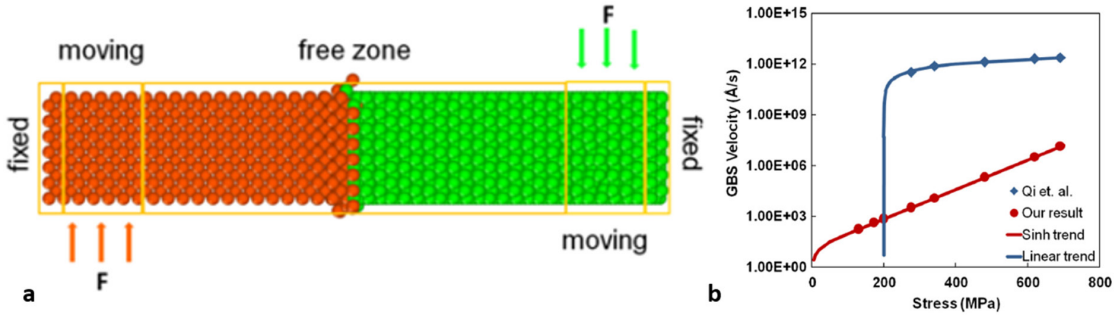

Figure 9. (a) Grain boundary sliding system set up; (b) grain boundary sliding constitutive law. Reprinted from [44] with permission. Copyright 2015 Elsevier.

applied to the moving zones of an Al bi-crystal. After the ABC sampling process, NEB and KMC were applied to obtain the most realistic mode of deformation, after which h-TST was used to calculate the transition time. From the grain boundary displacement and transition time, the corresponding grain boundary sliding velocity was evaluated. Thus, as figure 9(b) shows, the grain boundary sliding velocity can be obtained as a function of applied shear stress. The key conclusion of that work, as amply demonstrated in figure 9(b), is that slow strain rate ABC results and high strain rate MD results give very different sliding rates as a function of applied shear stress. Specifically, it was deduced that the grain boundary sliding constitutive law has a hyperbolic sine character and is highly non-Newtonian.

In both of these studies, ABC, in conjunction with a range of techniques, including NEB, KMC, and h-TST, were used to provide mechanistic details of atomistic deformation that cannot be obtained from classical MD simulations.

5.2. Applications of method 2: force-induced protein unfolding

For biologically-related problems, such as clamping force-induced protein folding and unfolding, it is a significant challenge for MD simulations to capture the entire unfolding process at experimental timescales. Because of this, the MD simulations of protein unfolding typically occur at clamping forces that are significantly larger and timescales that are significantly shorter than those seen experimentally. Because of this discrepancy in simulated and experimental timescales, atomistic resolution of the unfolding pathways and intermediate configurations that can directly be compared with experiments are generally lacking.

To this end, Park and co-workers [50–52] have applied method 2 of section 4 to study force-induced unfolding of the proteins ubiquitin, prion, and GFP. To illustrate the utility of this approach, we focus the present discussion on the unfolding of ubiquitin [50].

Figure 10 shows the unfolding times for ubiquitin as measured experimentally, and calculated using both method 2 as described above, and also SMD simulations. Importantly, figure 10 shows that the experimentally measured unfolding times are on the order of seconds, using clamping forces that are 200 pN and smaller. As can be seen, the SMD simulations

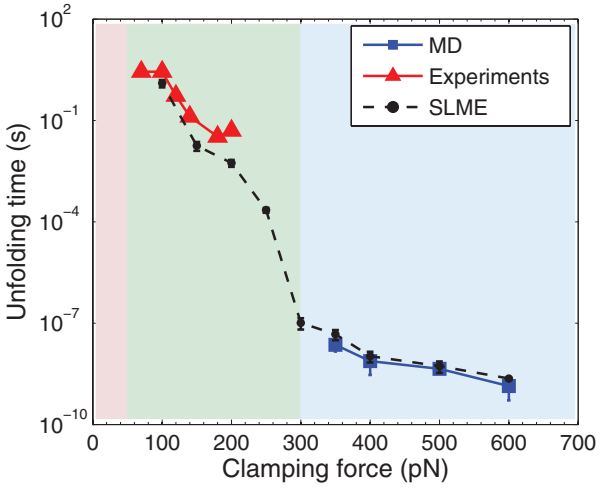

Figure 10. Unfolding time as a function of the clamping force for ubiquitin as obtained experimentally, using the ABC–SLME method, and also steered MD simulations [50].

are only able to simulate timescales up to about 10^{-7} s, or the microsecond timescale. In contrast, the ABC–SLME simulations are able to access both the high and low clamping force regimes, and agree well with both the high force SMD simulations, and the low force experiments. Most importantly, the ABC–SLME simulations capture the experimentally measured unfolding times of seconds when the clamping forces decrease below 200 pN. The ABC simulations also revealed new unfolding mechanisms and intermediate configurations that were not predicted experimentally, and revealed that the intermediate states were most likely not observed experimentally because their lifetimes are about two orders of magnitude smaller than the experimental temporal resolution [50].

5.3. Applications of method 3: diffusion of point defects in HCP Zr

Fan *et al* [19] adopted method 3 of section 4 (ABC-E) to study the anisotropic diffusion of point defects in HCP Zr. ABC-E allows the sampling of multiple transition pathways from a given minimum. Combined with on-the-fly KMC, Fan *et al* demonstrated multiple migration mechanisms for both interstitials and vacancies. They demonstrated that the

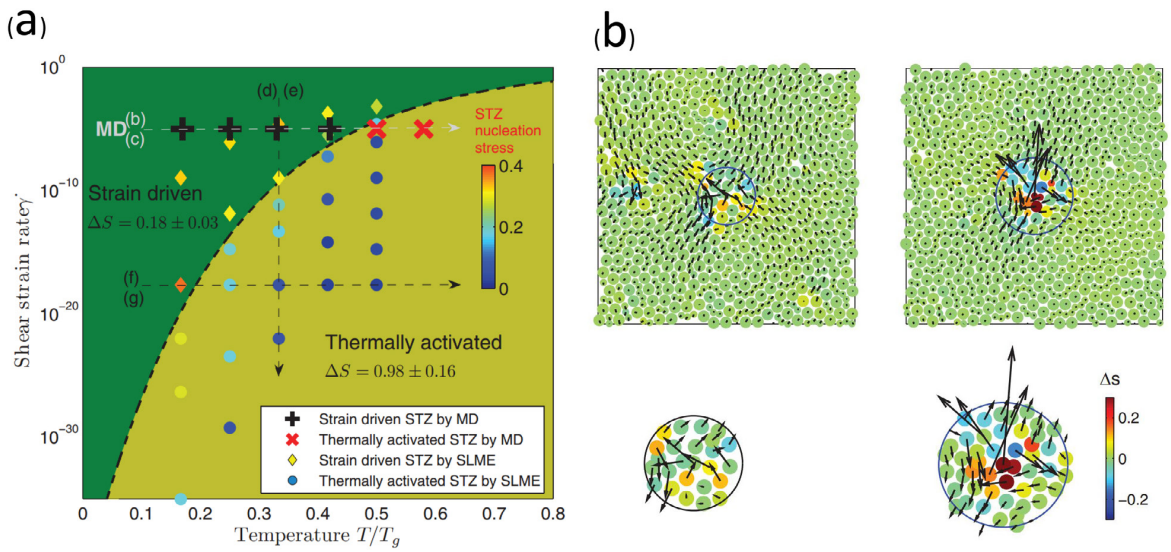

Figure 11. Two-dimensional BLJ strain-rate and temperature-dependence of deformation mechanism. (a) Summary of transition from strain-driven to thermally activated STZ nucleation as a function of strain rate and temperature, while also showing the dependence on the STZ nucleation stress, and the change in STZ area ΔS as computed using a Voronoi decomposition. (b) Change in Voronoi area ΔS of each atom between the undeformed configuration and STZ nucleation at T=0.33T_g for strain rates of (b) 2.4×10^{-5} and (c) 5.0×10^{-14}. Reprinted with permission from [56]. Copyright 2013 by the American Physical Society.

self-interstitial atom diffusion kinetics show a maximum anisotropy at intermediate temperatures (400–700 K).

Fan *et al* [19] also performed an interesting and direct comparison with ART to determine the respective capabilities of ABC-E and ART in finding low energy saddle points. They did this through studying vacancy hopping in HCP Zr, where all of the 12 pathways are known *a priori*. In doing so, they found that ABC-E was able to both predict the correct order of all 12 pathways in terms of energetic preference, but also at much lower computational expense than ART, which was able to capture 10 of the 12 different pathways, thus demonstrating the capability of the ABC-E method as a computationally efficient and important sampling approach.

5.4. Applications of method 4: strain-rate and temperature-dependent deformation mechanisms in amorphous solids

After developing method 4 as described in the previous section, Cao *et al* studied strain-rate and temperature effects on the shear transformation zones (STZs) in two-dimensional [56] and three-dimensional bulk amorphous solids [39], as well as on surface shear transformation zones in two-dimensional finite thickness amorphous solid films [57]. The structure and properties of STZs are important aspects to study because they are the unit carriers of plasticity in amorphous solids [68], playing a similar role as dislocations in crystalline solids.

One of the key findings of these works is shown in figure 11. In (a), the deformation map for the two-dimensional amorphous BLJ solid is shown as a function of strain rate and normalized temperature, where the MD strain rate corresponds to 10^{-5}, and room temperature corresponds to about 0.3 T_g, where T_g is the glass transition temperature. As can be seen in (b), at room temperature and high MD strain rates, the STZs exhibit volume preserving, shear deformation. In contrast, as the strain rate drops about 10 orders of magnitude, corresponding to an experimentally-accessible strain rate, the characteristics of the STZs change markedly. Specifically, the STZ area increases about 33%, its displacement field decays much more rapidly in space, less stress is needed to nucleate the STZ, its characteristic quadrupolar symmetry is lost, and perhaps most interestingly, the deformation mechanism inside the STZ changes from shear to tension [56]. This example illustrates the powerful and interesting predictions of fundamental mechanical properties that can be made if slower strain rates can be used in atomistic computation.

5.5. Applications of method 5: strain-rate-dependent mechanical response of metals

Method 5 for applying a constant strain rate has also been used in multiple applications. In the work in which method 5 was developed, Fan *et al* [62] studied the mechanisms of dislocation–defect interactions in HCP Zr for shear strain rates ranging from $\dot{\epsilon} = 10^{-6}$ s^{-1} to $\dot{\epsilon} = 10^{6}$ s^{-1}. In doing so, as shown in figure 12, they found a novel strain-rate-dependent trigger mechanism. Specifically, at high strain rates and low temperatures, edge dislocations and SIA clusters were found to exhibit a recovery mechanism, while at low strain rates and high temperatures, a climb mechanism was observed. The high strain rate deformation mechanism was confirmed by classical MD simulations, while the low strain rate response is a new observation. This work is an example of how these slow strain rate atomistic methods yield new insights into the strain-rate-dependent deformation mechanisms in different materials.

Using a simple model of a metallic nano-pillar that is often the subject of experimental works, Yan *et al* [69] attempted to circumvent the timescale bottleneck of conventional MD and provide novel physical insights into the rate-dependence of the mechanical behavior of nanostructures. Inspired by the

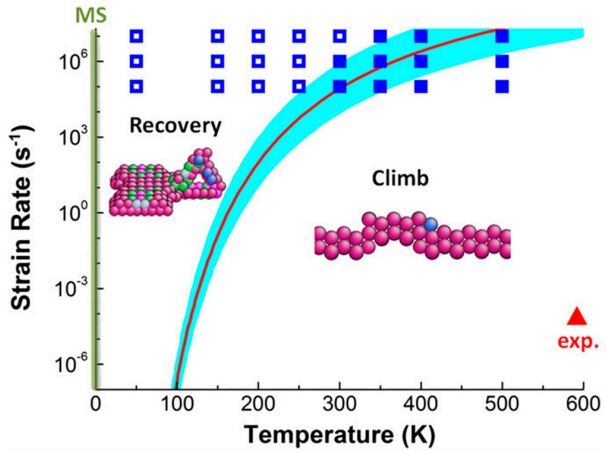

Figure 12. Strain-rate and temperature-dependence of recovery and climb mechanisms in dislocation–cluster interactions in HCP Zr. Reproduced with permission from [62]. Copyright 2013 National Academy of Sciences.

approach reported in [62], Yan *et al* [69] modified the approach described in method 5, and applied it to a study of Ni nanoslab compression. In the work of Fan *et al* [62], ABC was used to find a single new local energy minimum. In contrast, for the work of Yan *et al* [69], ABC sampling was continued until multiple local energy minima were found, at which point NEB was utilized to accurately calculate the energy barriers connecting the initial energy minimum to all the possible final configurations identified by ABC. KMC was then used to select the transition pathway, and h-TST was used to calculate the transition time (Δt) between the initial and selected final states.

The study of Ni nano-slab compression focused on investigating the deformation behavior and mechanisms under both experimentally-relevant (slow) and MD (fast) strain rates. While the high-strain rate deformation proceeds in an unremarkable manner, where the nano-slab shortens its length along with the formation of an expected defect sub-structure, the slow-strain-rate results, which are relevant to most applications and laboratory experiments, exhibit a dramatically different behavior. Specifically, liquid-like deformation at slow strain rates is observed, as shown in figure 13(b). *In situ* experiments [70] appear to qualitatively confirm the observations that nanostructures, indeed, are more likely to exhibit the deformation pattern captured with the slow-strain-rate timescaling approach in this research.

6. Key unresolved issues

The previous section, which highlighted a range of application areas, showed examples of how ABC can be a powerful tool in enabling the study of the behavior of atomistic systems over long timescales and at slow strain rates, both of which are not accessible to classical MD simulations. However, similar to any other numerical technique, there are still important unresolved issues with the ABC methods. In this section we therefore discuss these issues and offer, where relevant, possible solutions or paths forward.

6.1. Computational efficiency

The first and perhaps most important issue with the ABC methods is that of computational expense and efficiency. Ideally, these methods could be used interchangeably with classical MD, and thus could be used for atomistic systems containing hundreds of thousands, if not millions, of atoms. However, we are currently far from this objective. The key factor causing the computational expense of the ABC method can be shown through equation (3), where, to calculate the penalty function-modified potential energy $\Psi(\mathbf{r})$, a summation over all applied penalty functions p is required. This is problematic because, for the ABC method to explore the PES most efficiently, all previously applied penalty functions must be kept such that energy wells that have already been explored are not explored multiple times. While this makes the PES search more efficient, it also means that the computational expense associated with ABC increases as more of the PES is explored. Thus, the speed of the PES exploration is fairly good at the beginning of a typical ABC simulation, but decreases noticeably as more of the PES is explored.

Various issues have been developed to resolve this issue, which has limited the system sizes that can be studied using the ABC methodologies described in this work to a few tens of thousands of atoms. One obvious approach is to parallelize the ABC methodology, for example using an open source simulation code like LAMMPS, which has been done by both the Sharma and Park groups. However, because the ABC method also includes energy minimization after each penalty function is applied, the benefits of parallelization quickly decrease beyond a few nodes.

Another approach to alleviate this issue is to reduce the information stored in the memory, which can be realized in multiple ways. (1) By combining penalty functions, the ABC–SLME approach can significantly reduce the number of stored penalty functions and allow the system to explore more of the PES before the computational overhead becomes intractable [40]. (2) The PES exploration can be done in only localized regions of interest. For example, if the volume of the system where the phenomena of interest is localized or can be identified *a priori*, then only those portions of the PES associated with the atoms in the localized volume could be penalized [62, 69]. (3) Another approach would be to limit the number of penalty functions that are stored in memory; there would be some risk to this approach in that the system could still return to a previously explored energy well if the penalty functions were removed, but this could also be done by basing the decision to remove previously stored penalty functions on a criteria based on the distance away from previously explored energy wells on the PES.

6.2. PES resolution and penalty function parameter selection

Another issue of ABC is the resolution of the PES that is achieved, which, as shown in figure 14, depends on the heights and widths (or sizes) of the penalty functions. As shown in figure 14, if larger penalty functions ϕ_{p1} (red balls) are used, the PES that is effectively described is Φ_1. In contrast, if

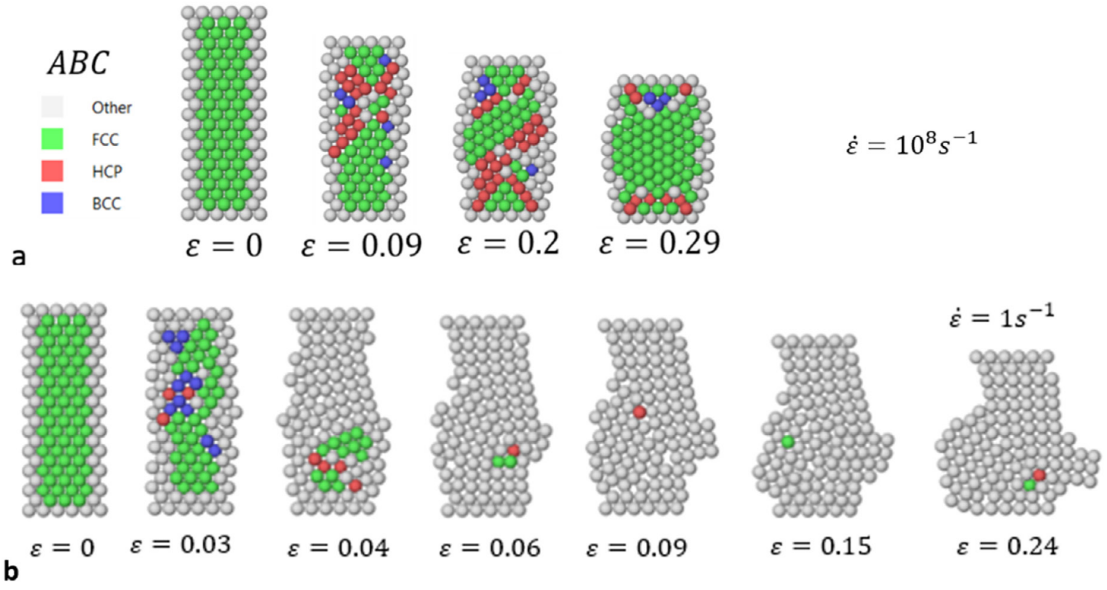

Figure 13. Ni compression under different strain rates. (a) Fast, MD-like strain rate. (b) Slow, experimentally-relevant strain rate. Reproduced with permission from [69]. Copyright 2016 American Chemical Society.

smaller penalty functions ϕ_{p2} (blue balls) are applied to the PES, the effective PES that is described is Φ_2.

If Φ_2 is the effective PES, then small-scale atomic motion, like the diffusion of atoms, can be captured. However, if the larger penalty functions leading to the effective PES described by Φ_1 are chosen, then only larger, more collective atomic motions, such as planar defects, may be captured, where we note that figure 14 is meant to be conceptually illustrative rather than quantitatively accurate. Therefore, the choice of the penalty function parameters can impact the physical phenomena that are observed in the simulations. This choice also impacts the computational efficiency. If the penalty functions are too large, the resolution may not be fine enough to capture the deformation, while if the penalty functions are too small, it will take a long time to explore a meaningful portion of the PES.

Unfortunately, there is currently no rigorous approach to quickly choosing the appropriate penalty function size and shape, and thus physical intuition and experience with both the ABC method as well as the physics of the problem of interest are required. This is particularly important for strain and strain-rate dependent phenomena, where the underlying PES evolves and changes with each strain increment, and thus where the penalty function parameters would need to dynamically evolve for each strain increment. Therefore, an approach that could identify the appropriate penalty function parameters based solely on the interatomic potential would be greatly beneficial.

This requirement is somewhat satisfied by the ABC–SLME method [40] as the penalty functions that result from the combination of multiple penalty functions are constrained in certain ways. Specifically, the ABC–SLME initializes new penalty function parameters after a true local energy minimum is explored. The penalty function width and height are determined by measuring the displacement and energy difference between a new local minimum and the corresponding saddle point. In this way, the penalty function parameters are self-determined and automatically updated according to the underlying PES.

6.3. Entropic effects

As has been established, the goal of the ABC method is to sample the PES. In doing so, this means that entropic effects, which contribute to the free energy of the system, are not accounted for, and thus the ABC method works best for problems in which the entropic effects do not dominate. This may be valid for lower temperature cases, or for applications where the PES barriers are sufficiently high such that entropy can be neglected, as the PES is temperature-independent. We note that while we have determined the ability of the ABC methods to access slow strain rate phenomena in amorphous solids [39, 56, 57], we have not, to-date, evaluated the performance of the ABC methodologies for soft amorphous materials like polymers.

In reality, the system moves from one basin to another with a rate that is dependent on the energy barrier between the two basins, as well as temperature, and thus entropic effects can be included via TST. For example, Fan *et al* [71] investigated the temperature dependence of an average vacancy cluster size of a bcc Fe system using TST and KMC based on configurations identified in ABC. The prediction of the cluster sizes using ABC and KMC was found to match experimental measurements. In this way, entropic effects can be somewhat accounted for through the KMC approach to choosing the trajectory along the PES. For other biologically-relevant problems, like protein unfolding, the difference between the free energy surface and the PES cannot be neglected. In these cases, umbrella sampling has been used to convert the information from the PES to that of a free energy [50, 51]. Such

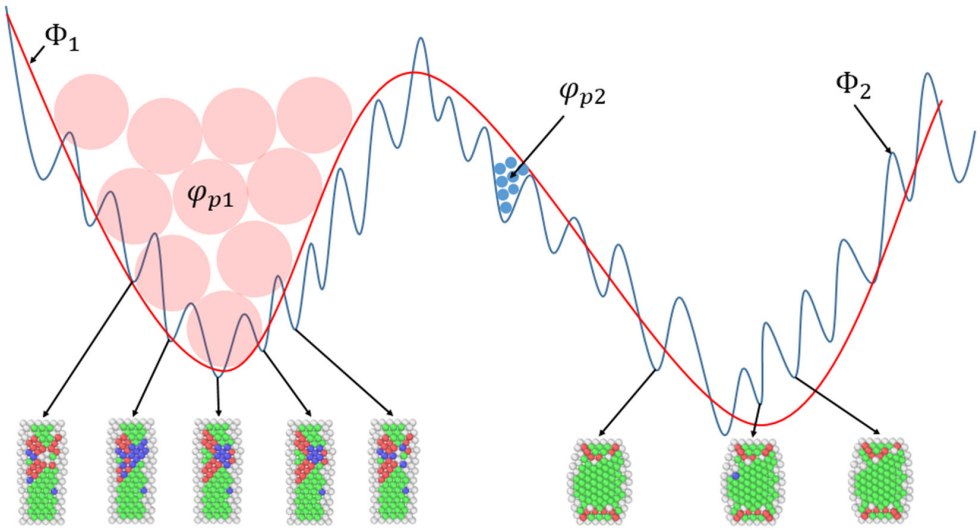

Figure 14. PES exploration with different penalty function resolutions. Note that the figure is meant to be conceptually illustrative rather than quantitatively accurate.

approaches can extend the validity of the ABC methodology, though a generic free energy-based search methodology would certainly be a long-term preferable alternative.

6.4. One-dimensional PES exploration

In the original ABC and ABC–SLME sampling, due to the manner in which the penalties are applied, the system does not return back to the energy well it has visited. In this way, the original ABC and ABC–SLME approaches [71, 72] ignore the appearance of other possible jumps from the current state. However, because this results in an incomplete catalog of possible transition states, it results in an overestimation of the transition times.

The time overestimation problem could be fixed through extending the searching dimensions, for example, ABC-E [19] (or other related methods like the dimer approach [16]). In this algorithm, after a new minimum is identified using ABC, a penalty is added on the saddle point to block the identified path. The system is then sent back to the initial state to find other possible minima around the initial state. The way ABC-E is adopted to search multiple transition paths is quite similar to ART [14] and the dimer approach [16].

There are advantages and disadvantages for both searching methods. A benefit of the one-dimensional search is that more states on the PES are explored, which may enable the observation of a dominant transition pathway or physical mechanism, while neglecting other, potentially less important, transition paths. These one-dimensional searching methods are also more efficient. However, ignoring the existence of other possible (i.e. higher energy) exit pathways has been shown to lead to overestimations of the calculated transition time out of an energy well [19, 72, 73].

ABC-E and other similar searching algorithms, such as dimer or ART, can identify multiple possible transition pathways out of a given energy well, which in our experience is particularly important for diffusion-based problems, where there are many competing states and pathways. However, the additional computational expense entailed in cataloging multiple transition pathways can be prohibitive. For example, in recent studies of the annihilation of dislocation dipoles, the ART method was unable to complete the simulations, while ABC was able to observe the dislocation dissociation processes [74, 75]. These issues again illustrate the need for more efficient ways to perform ABC-based explorations of the PES.

6.5. Length scale limitations

As we have discussed in this review, the various ABC methods have been effective in addressing the timescale issues that traditionally arise in classical MD simulations. However, in doing so, because of the limitations in the number of atoms (i.e. tens of thousands) that can be considered, the ABC methods are, at present, length scale limited. This length scale limitation also limits the types of problems that can be tackled using ABC, and thus the physical phenomena that are most often studied (as shown in this review) are those with localized unit processes, like diffusion and localized plastic deformation.

One approach that may be beneficial to extending the length scales of the ABC simulations is to use coarse-grained atomistic potentials, i.e. [76]. Using such potentials would enable the study of significantly larger length scales and system sizes with the same number of degrees of freedom, while potentially opening up the study of more complex system mechanics.

7. Concluding remarks

In this review, we discuss the application of a class of approaches centered around the so-called ABC method to circumvent the timescale bottleneck of traditional MD, with

particular emphasis on mechanically-driven problems at experimentally relevant strain rates and timescales. Our conclusion is perhaps no different than that for other competing approaches: there is currently no magic solution to bridging timescales. However, when armed with good physical intuition, the ABC method, when appropriately complemented with other algorithms and techniques (as described in the review) can yield useful information and novel insights into the rate-dependent mechanical behavior for materials science problems of interest.

Acknowledgments

XY and PS acknowledge support from NSF CMMI grants CMMI-1161163 and CMMI-1463205. HSP, PC and WT acknowledge the support of NSF CMMI-1234183.

References

[1] Taylor G I 1934 *Proc. R. Soc.* A **145** 362–87
[2] Bulatov V and Cai W 2006 *Computer Simulations of Dislocations* vol 3 (Oxford: Oxford University Press)
[3] Tadmor E B and Miller R E 2011 *Modeling Materials: Continuum, Atomistic and Multiscale Techniques* (Cambridge: Cambridge University Press)
[4] Yamakov V, Wolf D, Phillpot S and Gleiter H 2002 *Acta Mater.* **50** 61–73
[5] Van Swygenhoven H, Spaczer M, Caro A and Farkas D 1999 *Phys. Rev.* B **60** 22
[6] Cui Z, Gao F, Cui Z and Qu J 2012 *J. Power Sources* **207** 150–9
[7] Kushima A, Lin X, Li J, Eapen J, Mauro J C, Qian X, Diep P and Yip S 2009 *J. Chem. Phys.* **130** 224504
[8] Kushima A, Eapen J, Li J, Yip S and Zhu T 2011 *Eur. Phys. J.* B **82** 271–93
[9] Perez D, Uberuaga B P, Shim Y, Amar J G and Voter A F 2009 *Annu. Rep. Comput. Chem.* **5** 79–98
[10] Voter A F, Montalenti F and Germann T C 2002 *Annu. Rev. Mater. Res.* **32** 321–46
[11] Perez D, Uberuaga B P and Voter A F 2015 *Comput. Mater. Sci.* **100** 90–103
[12] Laio A and Parrinello M 2002 *Proc. Natl Acad. Sci.* **99** 12562–6
[13] Laio A and Gervasio F L 2008 *Rep. Prog. Phys.* **71** 126601
[14] Barkema G and Mousseau N 1996 *Phys. Rev. Lett.* **77** 4358
[15] Mousseau N and Barkema G 1998 *Phys. Rev.* E **57** 2419
[16] Henkelman G and Jónsson H 1999 *J. Chem. Phys.* **111** 7010–22
[17] Cances E, Legoll F, Marinica M C, Minoukadeh K and Willaime F 2009 *J. Chem. Phys.* **130** 114711
[18] Rodney D, Tanguy A and Vandembroucq D 2011 *Modelling Simul. Mater. Sci. Eng.* **19** 083001
[19] Fan Y, Yip S and Yildiz B 2014 *J. Phys.: Condens. Matter* **26** 365402
[20] Wales D J 2002 *Mol. Phys.* **100** 3285–305
[21] Wales D J 2004 *Mol. Phys.* **102** 891–908
[22] Carr J M and Wales D J 2008 *J. Phys. Chem.* B **112** 8760–9
[23] Carr J M and Wales D J 2005 *J. Chem. Phys.* **123** 234901
[24] Pattamatta S, Elliott R S and Tadmor E B 2014 *Proc. Natl Acad. Sci.* **111** E1678–86
[25] Hanggi P, Talkner P and Borkovec M 1990 *Rev. Mod. Phys.* **62** 251–342
[26] Voter A F 2007 Introduction to the kinetic Monte Carlo method *Radiation Effects in Solids* (Berlin: Springer) pp 1–23
[27] Henkelman G and Jonsson H 2000 *J. Chem. Phys.* **113** 9978–85
[28] Voter A F 1997 *Phys. Rev. Lett.* **78** 3908
[29] So M R *et al* 2000 *J. Chem. Phys.* **112** 9599–606
[30] Voter A F 1998 *Phys. Rev.* B **57** R13985
[31] Hamelberg D, Mongan J and McCammon J A 2004 *J. Chem. Phys.* **120** 11919–29
[32] Miron R A and Fichthorn K A 2003 *J. Chem. Phys.* **119** 6210–6
[33] Hara S and Li J 2010 *Phys. Rev.* B **82** 184114
[34] Chakraborty S, Zhang J and Ghosh S 2016 *Comput. Mater. Sci.* **121** 23–34
[35] Kushima A, Lin X, Li J, Qian X, Eapen J, Mauro J C, Diep P and Yip S 2009 *J. Chem. Phys.* **131** 164505
[36] Fan Y, Kushima A and Yildiz B 2010 *Phys. Rev.* B **81** 104102
[37] Fan Y, Yildiz B and Yip S 2013 *Soft Matter* **9** 9511–4
[38] Tang X Z, Guo Y F, Fan Y, Yip S and Yildiz B 2016 *Acta Mater.* **105** 147–54
[39] Cao P, Lin X and Park H S 2014 *J. Mech. Phys. Solids* **68** 239–50
[40] Cao P, Li M, Heugle R J, Park H S and Lin X 2012 *Phys. Rev.* E **86** 016710
[41] Ren W and Vanden-Eijnden E 2005 *J. Phys. Chem.* B **109** 6688–93
[42] Sheppard D, Terrell R and Henkelman G 2008 *J. Chem. Phys.* **128** 134106
[43] Yan X, Gouissem A and Sharma P 2015 *Mech. Mater.* **91** 306–12
[44] Gouissem A, Sarangi R, Deng Q and Sharma P 2015 *Comput. Mater. Sci.* **104** 200–4
[45] Popa I, Kosuri P, Alegre-Cebollada J, Garcia-Manyes S and Fernandez J M 2013 *Nat. Protocols* **8** 1261–76
[46] Perez-Jimenez R *et al* 2011 *Nat. Struct. Mol. Biol.* **18** 592–6
[47] Garcia-Manyes S, Liang J, Szoszkiewicz R, Kuo T L and Fernández J M 2009 *Nat. Chem.* **1** 236–42
[48] del Rio A, Perez-Jimenez R, Liu R, Roca-Cusachs P, Fernandez J M and Sheetz M P 2009 *Science* **323** 638–41
[49] Neuman K C and Nagy A 2008 *Nat. Methods* **5** 491–505
[50] Cao P, Yoon G, Tao W, Eom K and Park H S 2015 *Sci. Rep.* **5** 8757
[51] Tao W, Yoon G, Cao P, Eom K and Park H S 2015 *J. Chem. Phys.* **143** 125101
[52] Cao P, Tao W and Park H S 2016 *Extreme Mech. Lett.* **8** 251–6
[53] Park H S, Gall K and Zimmerman J A 2006 *J. Mech. Phys. Solids* **54** 1862–81
[54] Yamakov V, Wolf D, Phillpot S R, Mukherjee A K and Gleiter H 2002 *Nat. Mater.* **1** 1–4
[55] Belytschko T, Xiao S P, Schatz G C and Ruoff R S 2002 *Phys. Rev.* B **65** 235430
[56] Cao P, Park H S and Lin X 2013 *Phys. Rev.* E **88** 042404
[57] Cao P, Lin X and Park H S 2014 *Phys. Rev.* E **90** 012311
[58] Zhu T, Li J, Samanta A, Leach A and Gall K 2008 *Phys. Rev. Lett.* **100** 025502
[59] Ryu S, Kang K and Cai W 2011 *Proc. Natl Acad. Sci.* **108** 5174–8
[60] Johnson W L and Samwer K 2005 *Phys. Rev. Lett.* **95** 195501
[61] Cheng Y Q and Ma E 2011 *Acta Mater.* **59** 1800–7
[62] Fan Y, Osetskiy Y N, Yip S and Yildiz B 2013 *Proc. Natl Acad. Sci.* **110** 17756–61
[63] Stevenson J D and Wales D J 2014 *J. Chem. Phys.* **141** 041104
[64] Wales D J 2009 *J. Chem. Phys.* **130** 204111
[65] Lau T T, Kushima A and Yip S 2009 An atomistic method for slow structural deformations *IOP Conf. Ser.: Mater. Sci. Eng.* **3** 012002

[66] Lau T T, Kushima A and Yip S 2010 *Phys. Rev. Lett.* **104** 175501
[67] Plimpton S 1995 *J. Comput. Phys.* **117** 1–19
[68] Schuh C A, Hufnagel T C and Ramamurty U 2007 *Acta Mater.* **55** 4067–109
[69] Yan X and Sharma P 2016 *Nano Lett.* **16** 3487–92
[70] Sun J, He L, Lo Y C, Xu T, Bi H, Sun L, Zhang Z, Mao S X and Li J 2014 *Nat. Mater.* **13** 1007–12
[71] Fan Y, Kushima A, Yip S and Yildiz B 2011 *Phys. Rev. Lett.* **106** 125501
[72] Brommer P and Mousseau N 2012 *Phys. Rev. Lett.* **108** 219601
[73] Fan Y, Kushima A, Yip S and Yildiz B 2012 *Phys. Rev. Lett.* **108** 219602
[74] Wang H, Xu D, Rodney D, Veyssière P and Yang R 2013 *Modelling Simul. Mater. Sci. Eng.* **21** 025002
[75] Wang H, Xu D and Yang R 2014 *Modelling Simul. Mater. Sci. Eng.* **22** 085004
[76] Hsu D D, Xia W, Arturo S G and Keten S 2014 *J. Chem. Theory Comput.* **10** 2514–27